Polish Journal of Chemical Technology, 26, 4, 25—33, 10.2478/pjct-2024-0036

Impact of Structure Parameters on the Critical Performance of a Novel Calciner—A DEM-Based Study

Tiezhuang Zhou[1, 2], Fagen Zhang[3], Run Xu[1], Yan Gao[2], Genghua Xie[4], Kai Xiao[4], Bin Yang[1*], Wenchun Jiang[1*]

[1]College of New Energy, China University of Petroleum (East China), Qingdao, Shandong, 266580, China
[2]National Research Center for Drying Technology and Equipment Engineering Technology, Tianhua Chemical Machinery and Automation Institute Co., Ltd., Lanzhou, Gansu, 730060, China
[3]Wanhua Chemical Group Co., Ltd, Yantai, 215634, China
[4]Sinopec Catalyst Co., LTD. Changling branch, Yueyang, 414022, China
[*]*Corresponding author:* e-mail: b20150016@s.upc.edu.cn

Fracture in a revolving tube due to creep deformation and thermal-mechanical fatigue is a growing concern in industrial equipment research and production, especially after long-term exposure to corrosion and high-temperature conditions in roasting furnaces. The calcination temperature and residence time are crucial in the catalyst production process, with optimal conditions en-hancing catalyst activity and stability. To improve the longevity of roasting furnaces, optimizing the construction structure of the calciner is critical. This study develops a novel calciner structure and mathematical models to understand the effect of structural parameters on critical performance. Computer simulations, predictive modelling, and rotational velocity analysis of the novel calciner were performed using a DEM. The effects of the baffle angle and overlap ratio on the flow pattern and MRT were studied through simulations and experiments. The main conclusions are as follows: (1) The operating parameter with the greatest effect on the MRT was the rotational angular velocity, followed by the baffle angle and overlap ratio. (2) The MRT calculation based on the numerical method model showed an error of no more than 10.0% compared to the actual measurement data, confirming the model's accuracy. Our study provides a theoretical foundation for a deeper understanding of the complex MRT and flow field processes within this novel calciner. It also aids in optimizing the working parameters, performance, and structure of pilot equipment while offering fundamental data for future industrial applications.

Keywords: Novel calciner, Structure, Motion, Residence time, Discrete element method.

INTRODUCTION

Roasting furnaces are widely used in the chemical and metallurgical industries as continuous solid-handling reactors. They can be utilized for various purposes, such as heating, drying, calcination, and reactions involving different materials[1, 2]. Feedstock roasting is a vital step in catalyst production, where the moisture content decreases and the structure undergoes significant changes, resulting in a catalyst characterized by excellent chemical stability, a large surface area, and high catalytic activity[3].

In the field of industrial equipment research and production, there is growing concern regarding the occurrence of fractures in the revolving tubes of roasting furnaces. These fractures are caused by creep deformation and thermal-mechanical fatigue after extended periods of operation under corrosive and high-temperature conditions. Considerable research has been conducted on enhancing the performance and longevity of revolving tubes under extreme temperature conditions during the calcination process. These findings indicate that creep fractures typically occur at weld seams and are susceptible to corrosion (Fig. 1)[4, 5, 6, 7, 8, 9, 10].

Meanwhile, the temperature and residence time during calcination are crucial factors in the catalyst production process. Optimal calcination conditions are important for producing catalysts with high activity and stability. However, excessively long residence times can lead to structural defects and energy waste[11]. The most efficient catalyst calcination involves minimizing the residence time of particles in the calciner and optimizing the calcination temperature[12].

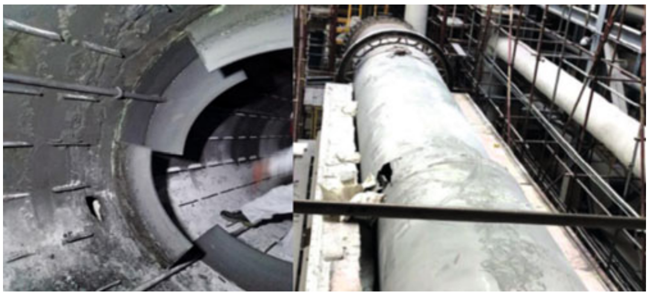

Figure 1. Diagram of the fracture location of the revolving tube

Previous research has developed theoretical models to predict the effects of particle properties and operating conditions on residence times in rotary kilns. A continuum model based on a single parameter was developed to predict the mean residence time (MRT) for cylindrical zeolite catalytic pellets in a rotary calciner. Experimental studies have been conducted to investigate the effects of feed rate, inclination angle, and rotational speed on residence time. At low fill levels, the residence time primarily depends on the bulk mean axial velocity[13]. Chatterjee et al. developed an empirical model for calculating the MRT for drums with low fill levels.

$$RT = \frac{0.1063 \cdot L^3}{\dot{V}} \cdot \left(\frac{\Theta}{\beta}\right)^{1.054} \cdot \left(\frac{\dot{V}}{L^3 \cdot n}\right)^{0.981} \cdot \left(\frac{L}{D}\right)^{1.1} \quad (1)$$

where Θ is the angle of repose, β is the angle of inclination of the rotary kiln, L is the length of the kiln, n is the rotational speed of the kiln, D is the internal diameter of the kiln, and $\dot{V}$ is the volumetric feed rate. Accordingly, the MRT is proportional to $\left(\frac{\theta}{\beta}\right)^{1.054}$ and the size ratio $\left(\frac{L}{D}\right)^{1.1}$ and inversely proportional to the rotation speed (n) and volumetric feed rate ($\dot{V}$). Saiah and Sahil[14] conducted measurements of MRT and axial dispersion ratios and compared the experimental results with values obtained from existing models. They observed that the rotation speed and rotary incline are the most influential factors affecting the MRT, while the feed rate has a marginal effect on the axial dispersion and MRT.

To study the residence time and heat transfer in rotary calciners, simulation techniques and numerical modelling have been developed[15, 16, 17] and heat transfer[18, 19] of rotary calciners. Previous studies have proposed empirically relevant factors related to the residence time and heat transfer ratio under various operating conditions. However, these theoretical models cannot be easily applied to different equipment calciners. Furthermore, their extension to other fields without experimental verification is risky and may limit their applications. Additionally, the models do not consider the influences of particle–surface and particle–particle interactions. While many methods utilize discrete element method (DEM) models to simulate the flow characteristics and heat transfer performance in the calciner, continuum modelling methods[20].

DEM simulations have been verified to be consistent with the experimental results of granular flows involving irregularly shaped particles[21, 22, 23, 24, 26] and rotating cylinders with different baffle shapes[27, 28]. In the DEM model, each constituent particle is considered to be a discrete independent motion element. The interactions between particles and boundaries, as well as the interactions among the particles themselves, are explicitly accounted for. Therefore, it is an effective method for analysing particle flow.

To improve the longevity of roasting furnaces, it is crucial to optimize the structural design of the calcinatory. In this study, a novel calciner structure and mathematical models are developed to investigate the effect of structural parameters on the critical performance of the novel calciner. However, most previous studies have focused primarily on granular flow in rotating calciners. There is limited or insufficient information available regarding the flow characteristics of particles in novel calciners. In this study, we evaluate the granular flow in a continuous novel calciner, with an emphasis on characterizing the flow under different operating conditions and baffles. The objective of this study is to establish and develop a predictive model through experiments and numerical simulations using DEM techniques. We investigate the effects of the blade type, operating conditions, and geometric design on the MRT. The experimental data from the same novel calciner are utilized to validate the results.

DEVELOPED EQUIPMENT AND ITS ADVANTAGES

As depicted in Fig. 2, a novel calciner system is formed by a feed tank, a rotary supply valve, a heating tube, a thermometer, a large plate, a small plate, and a product collection tank. Fig. 2 illustrates the three-dimensional structure of the calciner, which measures 2.1 m in length and 1.1 m in internal diameter. The calciner contains three small plates with external baffles and four large plates with internal baffles, arranged in alternating sequences within its interior. The procedure begins with the introduction of the treated catalyst into the top of the calciner, from which it descends onto the first large plate. The rotating plate and baffles are securely fixed to the shell housing, facilitating the spiral conveyance of the product across the heated plates towards the internal rim. Subsequently, the product descends from the inner hole to the small plate positioned below, where it is conveyed towards the outer edge. It then continues its descent to the lower large plate, propelled towards the inner edge by the continuous rotation of the plate. This flow pattern repeats throughout the height of the novel calciner until the product eventually exits from the bottom.

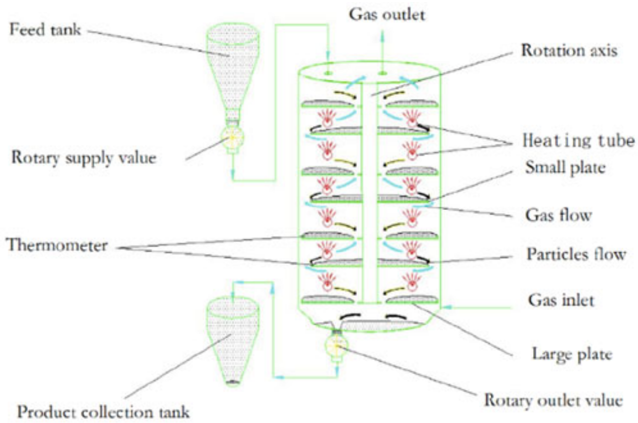

Figure 2. Development of a novel roasting system

The presented novel structure calciner offers several advantages over traditional roasting furnaces: (1) the tube, located in the low-temperature zone, remains stationary, and (2) the tube does not come into direct contact with the particles or corrosive gases, thereby preventing fracture of the calciner. However, accurately predicting the motion and residence time of particles within the novel calciner poses a challenge. Gaining a deeper scientific understanding of particle motion and residence time in this calciner will yield valuable insights into the calcination processes that involve heat exchange between the particles and the heated plate, as well as the high-temperature freeboard gas.

COMPUTATIONAL STUDY

Simulation Method

The granular flow process in the novel calciner model system was realized by using the DEM 2021. Our simulation focuses on catalyst granular flows in the novel Calciner using the Hertz–Mindlin (no slip) method, which accounts for various interactions, including particle-particle, particle–wall, and particle–baffle interactions. The simulation parameters for the Hertz–Mindlin (no-slip) method are presented in Table 1[29, 30].

Table 1. DEM Simulation Parameters

Item	Magnitude
Poisson's ratio	54 μm
Density	930 kg/m^3
Friction coefficient	0.3
Restitution coefficient	0.9

To facilitate the simulation results, computer-aided drawings of the novel calciner, including the first and second trays, the rotation axis, and baffles, were generated using SolidWorks 2020 software. A feeder was positioned at the calciner inlet to ensure a constant supply of particles at a uniform feed rate (Fig. 3). In the model, five baffles with widths, heights, and lengths of 4 mm, 60 mm, and 110 mm, respectively, were attached to the upper wall of the first tray. These baffles were implemented to enhance mixing and modify the flow path. The shape of the baffle was identical to that of another baffle immobilized by the inner wall of the calciner. We investigated the impact of the baffle size and angle α on the performance of the novel calciner. Specifically, the baffles were positioned at angles α (45, 50, and 55) with respect to the axis of the calciner. The tray rotation direction was clockwise when viewed along the axis of the rotation plate from the feed end. Integration times of 1e–12 s and overlap ratios of 5%, 10%, and 15% were utilized. The baffle sizes and angles (α) are listed in Table 2.

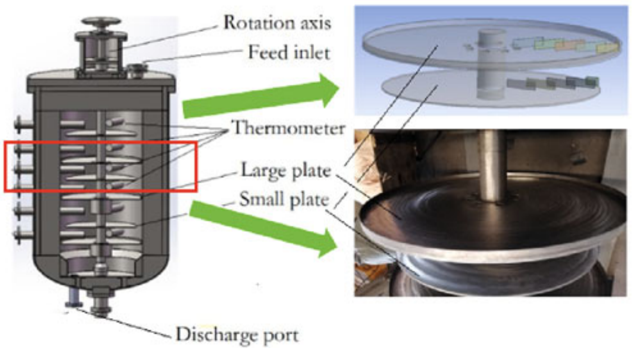

Figure 3. Simulation of a continuous novel calciner blender and calciner

Table 2. Baffle Blade Patterns

Baffle Pattern Name	Angle α (°)	Overlapping ratio (%)
Pattern Ⅰ	45	5%
Pattern Ⅱ	45	10%
Pattern Ⅲ	45	15%
Pattern Ⅳ	40	15%
Pattern Ⅴ	50	15%

To analyse the MRT of the product more accurately, a virtual receiving tank was installed below the small plate. In the normal working state, the product was continuously conveyed in the calciner by combining it with a fixed baffle and anticlockwise plates. As the plates rotated, the product was collected in the receiving tank.

Numerical Methodology

Schlunder and Jiang J[31, 32] investigated the heat transfer mechanism of particle materials in stirred beds and plate dryers and established a particle heat transfer theory and penetration model. This model allows for the calculation of the drying rate in batch dryers. We used this particle transfer model for the computations performed in this study. The repose angle of the catalyst was assumed to be constant throughout the entire roasting procedure and could be measured experimentally. The particle trajectory above the large plate is depicted in Fig. 4. Fig. 4 illustrates the particle movement trajectory model of the plate. Five annular granular heaps were present corresponding to the five baffles that removed the particles from near the internal rim and pushed them to the external rim. The centerline of each granular heap was considered to coincide with one edge of the corresponding internal baffle, which could be assumed to be the projection of the top point of the annular granular heap. The granular heaps flowed from the external rim to the internal rim and descended to the bottom larger plate. Here, they were transferred again towards the internal edge with the rotation of the plate. In general, the flow of an annular heap is composed of two segments. One is from the position of the external baffle to the internal baffle in the rotation direction of the principal axis, where the particle trajectory is circular. The other had a smaller trajectory parallel to the baffle.

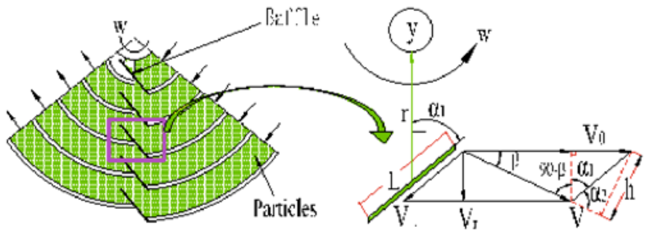

Figure 4. Particle movement model and particle trajectory near the baffle

This model considers the residence time, which is related to the number of baffles (n), length of the baffle (L), centre of the baffle radius (r), angular velocity (ω), and particle velocity. The resultant total residence time (τ) comprises the residence time of the small plate (τ_1) and that of the large plate (τ_2), as expressed by the following equations. Here, N1 and N2 represent the numbers of small and large plates, respectively, of the novel calciner.

The total particle velocity consists of the tangential velocity (vθ) along the ring and the parallel velocity (vr) along the baffle, and the triangular geometric relation of the particle velocity can be defined as:

$$v_\theta = r\omega \tag{2}$$

$$sin\beta = \frac{h}{v_\theta} = \frac{h}{\omega r} \tag{3}$$

$$\alpha_2 = 180 - (90 - \beta) = 90 - \alpha_1 + \beta \tag{4}$$

$$sin\alpha_2 = sin(90 - \alpha_1 + \beta) = \frac{h}{v_l} = cos(\alpha_1 - \beta) \tag{5}$$

Finally, by applying Eqs. (2), (3), (4) and (5), the velocity (vL) is written in Eq. (6):

$$v_l = \frac{\omega r sin\beta}{cos(\alpha_1 - \beta)} \tag{6}$$

The relation between v and vL can be written as:

$$v sin\beta = v_l cos\alpha_1 \tag{7}$$

The total velocity (v), tangential velocity (vθ) and parallel velocity (vr) can be calculated as:

$$v = \frac{v_l cos\alpha_1}{sin\beta} = \frac{\omega r cos\alpha_1}{cos\,(\alpha_1 - \beta)} \tag{8}$$

$$v_\theta = v\cos\beta = \frac{\omega r\cos\alpha_1\cos\beta}{\cos(\alpha_1-\beta)} \tag{9}$$

$$v_r = \frac{dr}{dt} = \frac{\omega r\cos\alpha_1\sin\beta}{\cos(\alpha_1-\beta)} \tag{10}$$

Taking an integral of the parallel velocity (vr) function yields the particle trajectory, r.

$$\int_{r_1}^{r}\frac{\cos(\alpha_1-\beta)}{\omega r\cos\alpha_1\sin\beta}dr = \int_0^t dt \tag{11}$$

The total particle trajectory can be mathematically expressed as:

$$r = \begin{cases} r_1 e^{\frac{wt\cos\alpha_1\sin\beta}{\cos(\alpha_1-\beta)}} & contact \\ r & non-contact \end{cases} \tag{12}$$

Similarly, the residence time of the particle consists of the contact time (τ_1') and noncontact time (τ_2') with the baffle:

$$\tau_1' = \frac{L}{V_L} = \frac{L\cos(\alpha_1-\beta)}{wr\sin\beta} \tag{13}$$

$$\tau_2' = \frac{2\pi}{w} \tag{14}$$

$$\tau_1 = N_1 n_1(\tau_1' + \tau_2') = N_1 n_1\left(\frac{L\cos(\alpha_1-\beta)}{wr\sin\beta} + \frac{2\pi}{\omega}\right) \tag{15}$$

where n_1 is the number of baffles. Similarly, the residence time of the particle above the small plate is calculated as:

$$\tau_2 = N_2 n_2\left(\frac{L_2\cos(\alpha_1-\beta)}{\omega r_2\sin\beta} + \frac{2\pi}{\omega}\right) \tag{16}$$

Therefore, the total mean residence time in the calciner is:

$$\tau = \tau_1 + \tau_2 = N_1 n_1\left(\frac{L_1\cos(\alpha_1-\beta)}{\omega r_1\sin\beta} + \frac{2\pi}{\omega}\right) + N_2 n_2\left(\frac{L_2\cos(\alpha_1-\beta)}{\omega r_2\sin\beta} + \frac{2\pi}{\omega}\right) \tag{17}$$

where α_1 is the baffle mounting angle (°), L is the baffle length (m), ω is the angular spin rate of baffle (s^{-1}), r is the distance between the material and axis (m), v_θ is the tangential velocity of the particles (m/s), v_r is the parallel velocity of the particles (m/s), and v is the total velocity of the particles (m/s).

Experimental Method of Mean Residence Time

The mean residence time and flow pattern were verified on a pilot-plant device. Experimental images of the catalyst flow pattern in the novel calciner are shown in Fig. 5. The experiments were conducted in an industrial pilot plant novel calciner with a geometry similar to that studied in the simulations. The experiments were carried out at atmospheric pressure and temperature. The calciner has dimensions of 2.1 m in length and 1.1 m in internal diameter. The calciner is equipped with three small plates with external baffles and four large plates with internal baffles installed inside, in alternating sequences. Fig. 5 illustrates the operating principle of the novel calciner. The treated catalyst is fed into the top of the calciner and falls onto the first large plate. The rotating plate and baffles are securely attached to the shell housing. This arrangement conveys the product in a spiral pattern across the heated plates towards the internal rim. Then, the product descends from the inner hole to the small plate located at a lower position. On this plate, the product is conveyed to the outer edge before descending to the lower large plate. Here, the product is conveyed towards the inner edge due to the continuous rotary motion of the plate. This flow pattern is repeated along the height of the novel calciner. Finally, the product flows out from the bottom of the calciner. A rotary valve is used to feed the catalyst into the calciner at a constant rate. The calciner is operated at various rotational angular velocities: 1, 1.5, 2, 2.5, and 3 rad/s. Overlapping ratios of 5%, 10%, and 15% RPM are applied. The calciner is equipped with several different baffles to adjust the angles to 40°, 45°, and 50°.

The MRT of the tracers is expressed as:

$$\tau = \int_0^\infty t\cdot E(t)\cdot d(t) \tag{18}$$

The can be mathematically expressed as

$$E(t) = \frac{C(t)}{\int_0^\infty t\cdot C(t)\cdot d(t)} \tag{19}$$

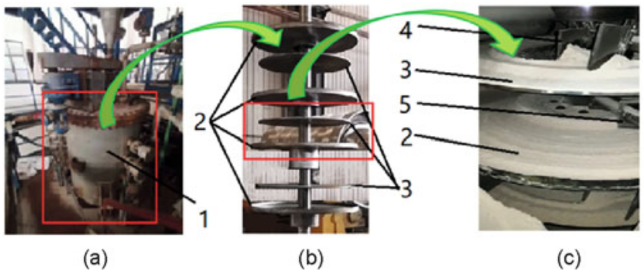

1-calciner; 2-large plate; 3-small plate; 4- external baffle; 5-internal baffle

Figure 5. The tracers and experimental images of MRTs

As shown in Fig. 6, the MRTs of the catalysts were measured at six rotational angular velocities: 1, 1.5, 2, 2.5, 3, and 3.5 rad/s. The results, also presented in Fig. 6, indicate that the MRT of the entire calciner (which contains 7 plates) decreased as the rotational speed increased. The calculated results based on the numerical methodology model consistently follow the

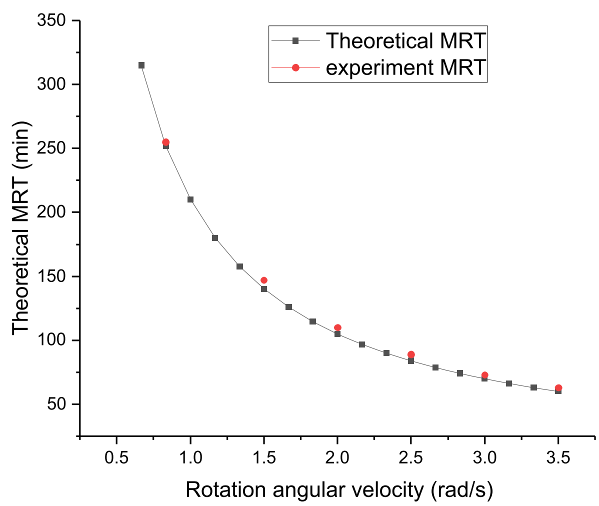

Figure 6. Comparison of the theoretical and experimental MRT values

same trend as the experimental data, with a relative error ranging from 4.0% to 10.0%. Throughout the calculation process, the calculated MRT using the numerical methodology model differed by no more than 10.0% from the actual measurement data, confirming the accuracy of the numerical methodology model in determining the mean residence time within the calcination process. These results demonstrate good agreement between the numerical and measured results.

RESULTS

Effect of the overlap ratio on the flow pattern

The effect of the overlap ratio on the flow pattern close to the baffle is shown in Fig. 7.

The simulation results revealed that when the overlap ratio, ξ, was 5%, most of the catalysts near the baffle moved towards the external edge of the plate, resulting in an increase in the MRT of the catalysts in the calciner. As the overlap ratio, ξ, increased to 10%, some portions of the catalysts continued to move towards the external edge of the plate. When the overlap ratio ξ increased from 10% to 15%, only a small portion of the catalysts moved in a direction opposite to the design flow direction. Increasing the overlap ratio was beneficial for accurately controlling the catalyst retention time. However, excessive increases led to a reduction in the catalyst retention time in the plate, necessitating more heating plates to ensure the desired retention time of the product in the calciner.

Effect of Baffle Angle on Flow Pattern

The effect of the baffle angle on the flow pattern is shown in Fig. 8.

The effect of the baffle angle on the flow pattern was found to be similar to that of the overlap ratio. None of the catalysts could be transferred to the inner granular

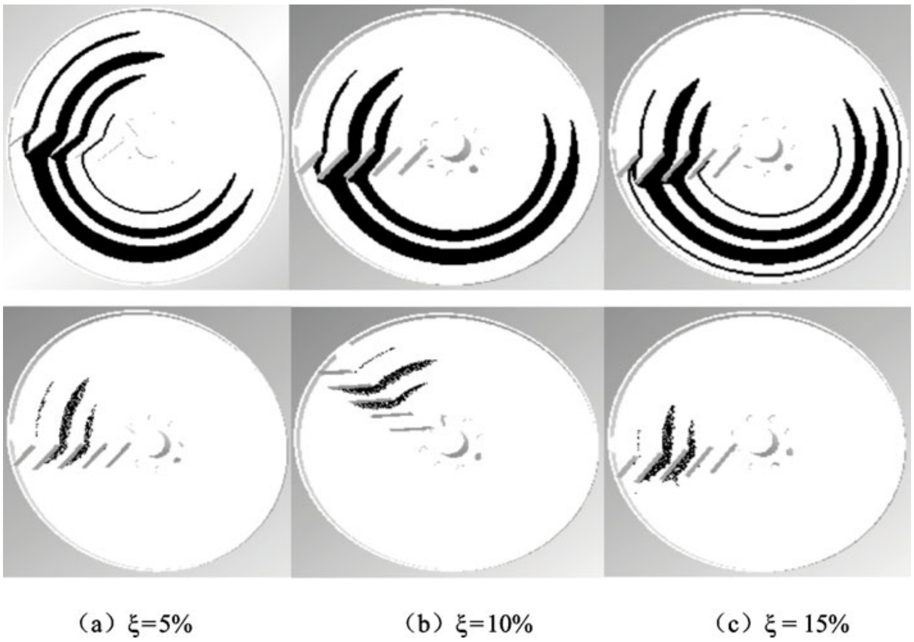

Figure 7. Effect of overlapping ratio design on flow pattern

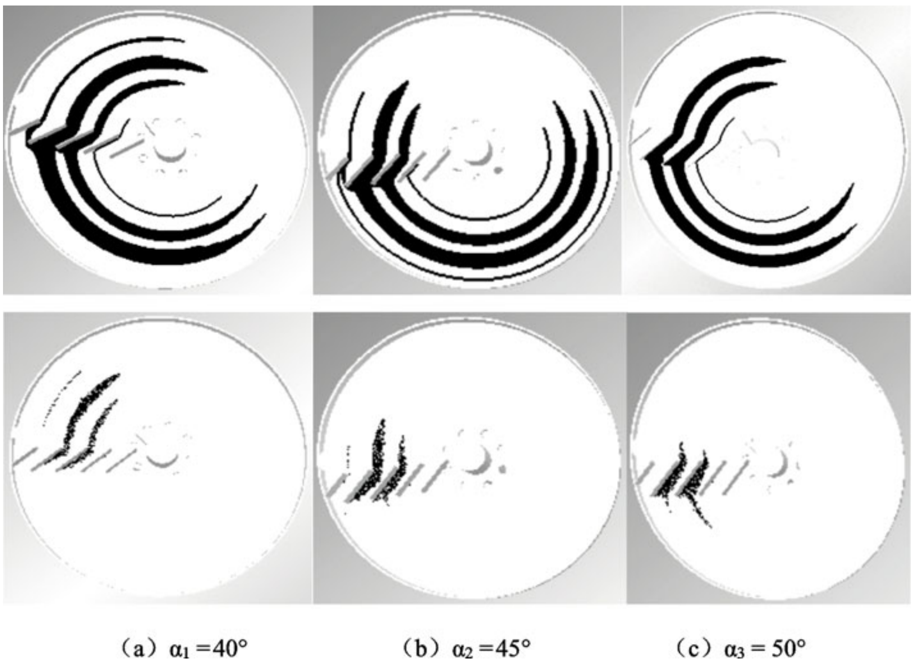

Figure 8. Effect of baffles angle design on flow pattern

heaps with a single rotation when the baffle angle α_1 was set at 40°. The flow pattern remained relatively unchanged between 40° and 45°, but a more pronounced effect was observed between 45° and 50°. Furthermore, an increased baffle angle resulted in fewer particles moving towards the external edge of the plate, ultimately bringing the calculation results closer to the desired conditions outlined in this study. By considering the overlap ratio and angle design of the baffle in combination, the optimal combinations of working parameters were determined to be a 15% overlap ratio (ξ) and a 50° baffle angle design (α_1). This research contributes to the development of geometric designs aimed at optimizing performance. The findings presented in this study can serve as a useful foundation for the future design and optimization of baffle structures for novel calciners.

Effect of the Baffle Structure on the MRT

The effect of different baffle overlap ratios (5%, 10%, and 15%) on the MRT is illustrated in Fig. 9(a). It is evident that the calciner output remained close to zero when the feed time was less than 82 min, primarily due to the lack of product flow into the receiving tank. As the MRT increased, the calciner output gradually improved. Notably, the MRT decreased with increasing baffle overlap ratio. Specifically, the MRTs were 107.9, 109.6, and 112.04 min for baffle overlap ratios of 5%, 10%, and 15%, respectively.

Fig. 9(b) depicts the behavior of the mean centered variance (σ2) in relation to the baffle overlapping ratios. As the baffle overlap ratio increased from 5% to 15%, the mean centered variance decreased, indicating that the baffle induced less dispersion at the higher overlap ratios of 10% and 15% compared to the 5% overlap ratio. A lower overlap ratio resulted in a greater amount of backmixing within the calciner, indicating a strong interaction between the mean-centered variance and the baffle structure. Based on the flow pattern analysis described in Section 4.2, it was found that the reversing flow of the partial product played a significant role in causing variations in the MRT.

The effect of varying the angle design (40°, 45°, and 50°) on the MRT is illustrated in Fig. 10(a). When the feed time was less than 75 min, the calciner output was ap-proximately 0 kg. The effect of the baffle angle on the MRT was similar to that of the overlap ratio, with an increase in the baffle overlap ratio resulting in a decrease in the MRT. However, the effect of varying the angle on the MRT was greater than that of varying the overlap ratio. Specifically, when the baffle angles were 40°, 45°, and 50°, the MRT values were 105.8, 107.9, and 109.4 min, respectively.

The mean centered variance decreased as the baffle angle increased from 40° to 50°, indicating that the baffle caused more dispersion at a 40° angle than at 10% or 15% (Fig. 10(b)). This observation was consistent

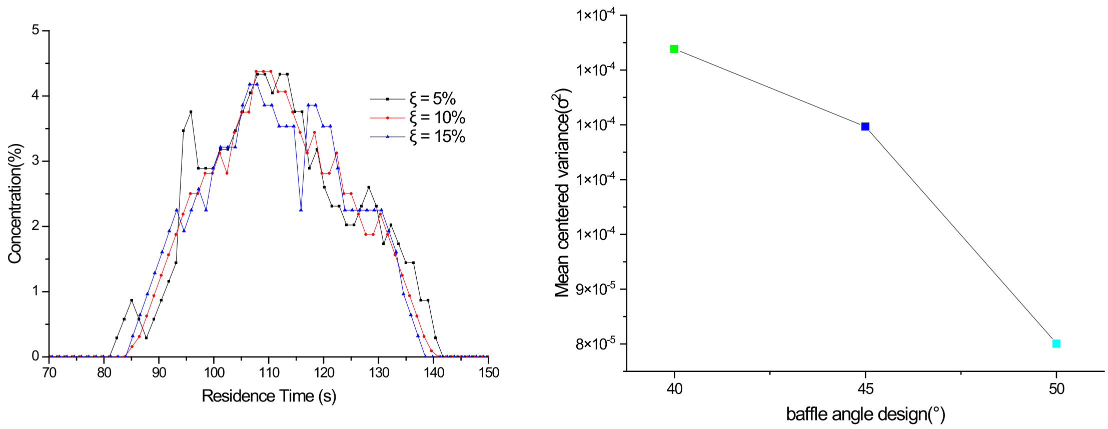

(a) (b)

Figure 9. Effect of the overlap ratio on the MRT and MCV

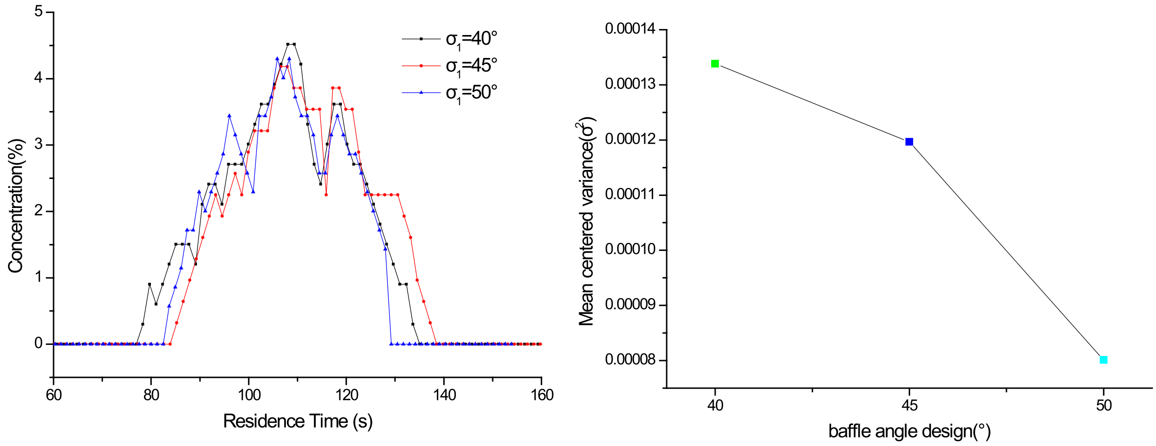

(a) (b)

Figure 10. Effect of baffle angle design on MRT and MCV

with the flow pattern analysis described in Section 3.3. Careful consideration must be given to the selection of an optimum baffle structure and the development of dynamic models for control purposes.

Effects of the Rotational Velocity and Feed Rate

During the motion of the novel calciner, the catalysts came into contact with the plate and baffle, which primarily determined the MRT of the product. The first factor was the contact time required for the products to flow along the baffle. The second factor was the time during which the product remained relatively static with plate rotation. The MRTs of the catalysts were calculated under five rotational angular velocities (0.5, 0.75, 1.0, 1.25, 1.5, 1.75, and 2.0 rad/s) and are shown in Fig. 11. Increasing rotational speeds resulted in a reduction in the MRT when the calciner was operating at different rotational velocities. This indicates that increasing the rotational speed caused the concentration function to shift noticeably to the left (Fig. 11(a)). However, the effect was minor at higher rotational speeds, as shown in Fig. 11(b).

At certain rotational speeds, the concentration distributions became narrower with increasing feed rate (Fig. 12). This implies that while the particles spent more time on average at lower feed rates, there was also greater variability in the amount of shear. This effect was less pronounced at higher speeds.

Comparison of Theoretical and Simulation Results

The responses derived from the simulation data and theoretical measurements were compared. As depicted in Fig. 13, the MRT decreased as the rotational angular

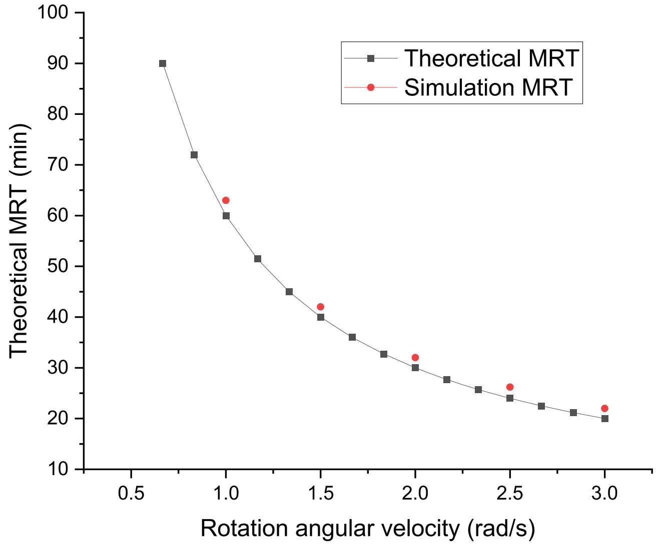

Figure 13. Comparison of the theoretical and experiment MRT values

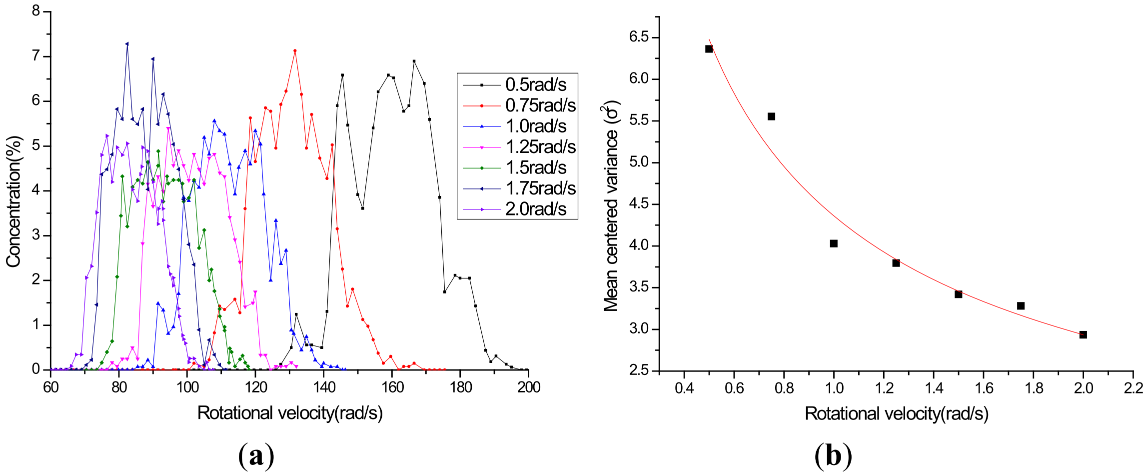

Figure 11. Effect of rotational velocity on MRT and MCV

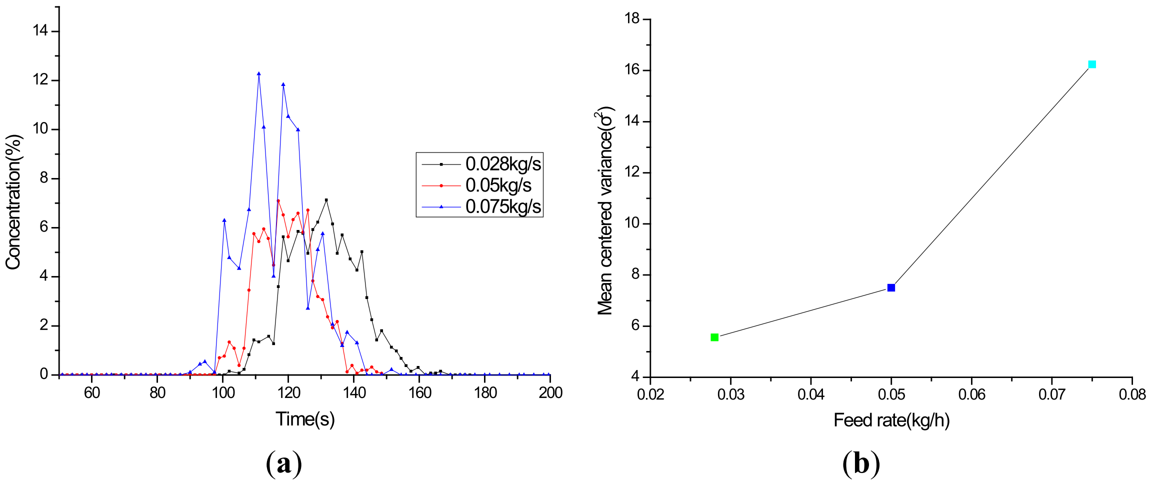

Figure 12. Effect of feed rate on MRT and MCV

velocity increased. Additionally, the decrease in MRT slowed at higher rotational angular velocities. Furthermore, the results indicated that the partially simulated MRT was consistent with the partially theoretical MRT of the calciner, which consists of two plates. Specifically, as the rotational speed increased from 0.67 rad/s to 3 rad/s, the MRT decreased significantly from 90.1 min to 22.3 min. Thus, the rotational angular velocity had a significant influence on the MRT compared to the previously mentioned theoretical and simulated MRT values.

CONCLUSION AND DISCUSSION

1) Computer simulations, predictive modelling, and rotational velocity analysis were conducted using the DEM to study a novel calciner. Simulations and experiments were performed to examine the effects of the baffle angle and overlap ratio on the flow pattern and MRT.

2) Among the operating parameters studied, the rotational angular velocity had the greatest influence on the MRT, followed by the baffle angle and overlap ratio.

3) The calculation of MRT, based on the numerical methodology model, demon-strated an error of no more than 10.0% compared to the actual measurement data. This confirms the accuracy of the numerical methodology model in predicting the mean residence time within the calcination process and indicates good agreement between the numerical and measured results.

Further investigation is needed to understand the effect of the feed rate on the flow pattern and MRT. Additionally, the influence of cohesion on the particle flow pattern, particularly on the MRT, should be explored further. While the material stud-ied in this work behaved similarly to free-flowing materials, it is necessary to conduct further experiments using different powders with varying moisture contents and par-ticle characteristics. Once a better understanding of the flow in novel calciners is ob-tained through motion studies, experiments should be conducted at high temperatures to study the effect of heat on material flow. This knowledge will contribute to optimiz-ing novel calciner processes.

Furthermore, this research provides a theoretical foundation for a more compre-hensive understanding of the complex MRT and flow field processes within this novel calciner. It also facilitates the optimization of the operational parameters, performance, and structure of pilot equipment while providing fundamental data for future studies in actual industrial applications.

ACKNOWLEDGMENTS

This research was supported by the National Key Research and Development Plan of China (No. 2022YFB3504000) and the Gansu Provincial Science and Technology Plan of the Major Project (No. 22ZD6GA024). We are grateful to Dr. Chengqing Wang for the effective discussions on rotary kiln transport processes. The contributions of Xiao Kai and Y. B. Xie to this study are gratefully acknowledged.

LITERATURE CITED

1. Zhao, J., Zhao, Q. & Zhao, Q. (2011). The new generation of vertical shaft calciner technology. John Wiley & Sons, Ltd. DOI: 10.1002/9781118061992.ch157.

2. Yang, Y., Gong, S., Ning, Q., Zhou, X. & Zhao, H. (2018). Development and application of electrocalciners with increased calcination temperature. In Light Metals, 1363–1371. DOI: 10.1007/978-3-319-72284-9_178.

3. Qi, L., Zhao, Z., Wang, R., Gao, W., Li, J. & Zhang, Y. (2020). Simultaneous Desulfurization and Denitrification Using La–Ce–V–Cu–ZSM-5 Catalysts in an Electrostatic Precipitator. ACS Omega. DOI: 10.1021/acsomega.0c00808.

4. Sinyavskii, D.P. & Gopkalo, A.P. (1979). Thermal fatigue of chromium-molybdenum steels used in sintering machine and roasting furnace components. Strength of Materials, 11(11), 1202–1205. DOI: 10.1007/bf00767041.

5. Lu, S., Zhang, P., Qin, C., Wang, X., Luo, F. & Zhou, J. (2006). The analysis on causes of rupture of a HP-NB high temperature alloy radiant furnace tube. In ASME Pressure Vessels and Piping Conference, 321–326. DOI: 10.1115/PVP2006-ICPVT-11-93008.

6. Ning, X.J., Cheng, S.S. & Xie, N.Q. (2009). Analysis of temperature, stress, and displacement distributions of staves for a blast furnace. *Internat. J. Minerals, Metal. Mater*. 16(5), 512–516. DOI: 10.1016/S1674-4799(09)60089-3.

7. Wang, H., Chen, Y., Xie, K., Wang, D. & Zhou, J., (2009). Strength and fatigue fracture analysis of the hydro--damper of a rotary kiln. *J. Mech. Strength*, 31(6), 992–998. DOI: 10.1061/41039(345)45.

8. Wen-Xi, D. & Ke-Zhong, S.(2006). Analysis of roasting furnace fracture and invalidation. Inner Mongolia Petrochemical Industry.

9. Hasan, A.M., Guo, S.M. & Wahab, M.A. (2009). Analysis of fracture in high-temperature vacuum tube furnace. *J. Failure Anal. Prev*. 9, 262–269. DOI: 10.1007/s11668-009-9236-z.

10. Rao, M.A., Babu, R.S. & Kumar, M.P. (2017). Failure investigation of a cooling coil tube in zinc roaster furnace. *Engin. Failure Anal.* 77, 118–125. DOI: 10.1016/j.engfailanal.2017.01.004.

11. Da Ros, S., Barbosa-Coutinho, E., Schwaab, M., Calsavara, V. & Fernandes-Machado, N.R. (2013). Modeling the effects of calcination conditions on the physical and chemical properties of transition alumina catalysts. *Mat. Character.* 80, 50–61. DOI: 10.1016/j.matchar.2013.03.005.

12. Helwani, Z., Ramli, M., Saputra, E., Putra, Y.L., Simbolon, D.F., Othman, M.R. & Idroes, R. (2020). Composite catalyst of palm mill fly ash-supported calcium oxide obtained from eggshells for transesterification of off-grade palm oil. *Catalysts*, 10(7), 724. DOI: 10.3390/catal10070724.

13. Sudah, O.S., Chester, A.W., Kowalski, J.A., Beeckman, J.W. & Muzzio, F.J. (2002). Quantitative characterization of mixing processes in rotary calciners. *Powder Technol*. 126(2), 166–173. DOI: 10.1016/S0032-5910(02)00009-8.

14. Chatterjee, A., Sathe, A.V. & Mukhopadhyay, P.K.. (1983). Flow of materials in rotary kilns used for sponge iron manufacture: part ii. effect of kiln geometry. *Metal. Transact*. B, 14(3), 383–392. DOI: 10.1007/BF02654357.

15. Chen, I.Y., Navodia, S., Yohannes, B., Nordeck, L., Machado, B., Ardalani, E. & Cuitiño, A.M. (2021). Flow of a moderately cohesive FCC catalyst in two pilot-scale rotary calciners: Residence time distribution and bed depth measurements with and without dams. Chem. Engin. Sci. 230, 116211. DOI: 10.1016/j.ces.2020.116211.

16. Pichler, M., Haddadi, B., Jordan, C., Norouzi, H. & Harasek, M. (2021). Influence of particle residence time distribution on the biomass pyrolysis in a rotary kiln. *J. Anal. Appl. Pyrol.* 158, 105171. DOI: 10.1016/j.jaap.2021.105171.

17. Mikulčić, H., Vujanović, M., Fidaros, D.K., Priesching, P., Minić, I., Tatschl, R. & Stefanović, G. (2012). The application

of CFD modelling to support the reduction of CO2 emissions in cement industry. *Energy*, 45(1), 464–473. DOI: 10.1016/j.energy.2012.04.030.

18. Chaudhuri, B., Muzzio, F.J. & Tomassone, M.S. (2010). Experimentally validated computations of heat transfer in granular materials in rotary calciners. *Powder Technol.* 198(1), 6–15. DOI: 10.1016/j.powtec.2009.09.024.

19. Tomassone, M.S., Chaudhuri, B. & Muzzio, F.J. Heat Transfer in Granular Flow in Rotary Calciners: Experiments and Particle Dynamics Simulations.

20. Chaudhuri, B., Muzzio, F.J. & Tomassone, M.S. (2011). Experimentally validated numerical modeling of heat transfer in granular flow in rotating vessels. Heat Transfer: Mathematical Modelling, Numerical Methods and Information Technology, 271–306.

21. Santos, D.A., Barrozo, M.A., Duarte, C.R., Weigler, F. & Mellmann, J. (2016). Investigation of particle dynamics in a rotary drum by means of experiments and numerical simulations using DEM. Advanced *Powder Technol*. 27(2), 692–703. DOI: 10.1016/j.apt.2016.02.027.

22. Iroba, K.L., Mellmann, J., Weigler, F., Metzger, T. & Tsotsas, E. (2011). Particle velocity profiles and residence time distribution in mixed-flow grain dryers. Granular Matter. 13, 159–168. DOI: 10.1007/s10035-010-0222-7.

23. Machado, M.V., Nascimento, S.M., Duarte, C.R. & Barrozo, M.A. (2017). Boundary conditions effects on the particle dynamic flow in a rotary drum with a single flight. *Powder Technol.*, 311, 341–349. DOI: 10.1016/j.powtec.2017.01.076.

24. Liu, J., Sysyn, M., Liu, Z., Kou, L., Wang, P. (2022).Studying the Strengthening Effect of Railway Ballast in the Direct Shear Test due to Insertion of Middle-size Ballast Particles. *J. Appl. Comput. Mech*. 1-11. DOI: 10.22055/jacm.2022.40206.3537.

25. Mahdavy, S., Norouzi, H.R., Jordan, C., Haddadi, B. & Harasek, M. (2022). Residence Time Distribution of Non-Spherical Particles in a Continuous Rotary Drum. *Processes*, 10(6), 1069. DOI: 10.3390/pr10061069.

26. Liu, X. Jiang, J. (2004). Mass and heat transfer in a continuous plate dryer. *Drying Technol*. 22(7), 1621–1635. DOI: 10.1081/DRT-200025619.

27. Schlünder, E.U. (1984). Heat transfer to packed and stirred beds from the surface of immersed bodies. *Chem. Engin. & Proces. Proces. Intensific.* 18(1), 31–53.

28. Keey, R.B. (1991). Drying of loose and particulate materials. CRC Press.

29. Wu, Guorong, Zhanfei, Zuo, and Yanggui, Li. (2023). "Selection of relative DEM time step for modelling fast fluidized bed of A-Type FCC particles." Symmetry 15.2, 488.

30.Wu, Guorong, Yanggui, Li, and Muhammad, Israr. (2023). "Improvement of relative DEM time step range in fast fluidization simulation of Type-A FCC particles." *Processes* 11.4, 1155.

31. Liu, X. & Jiang, J. (2004). Mass and heat transfer in a continuous plate dryer. *Drying Technol.* 22(7), 1621–1635. DOI: 10.1081/DRT-200025 619.

32. Zhang, J.J., Yang, D.C. & Li, J.R. (2011). Discussion on blade design of continuous plate dryer. *Chem. Engin.* (China), 39(3), 2. DOI: 10.3969/j.issn.1005-9954. 2011.03. 004.